

Competition between Thermal Fluctuations and Disorder in the Crystallization of ^4He in Aerogel

Ryuji Nomura, Aiko Osawa, Tomohiro Mimori, Ken-ichi Ueno, Haruko Kato, and Yuichi Okuda

Department of Condensed Matter Physics, Tokyo Institute of Technology, 2-12-1 O-okayama, Meguro, Tokyo 152-8551, Japan
(Received 25 July 2008; revised manuscript received 3 September 2008; published 23 October 2008)

The dynamical transition in the crystallization of ^4He in aerogel has been investigated by direct visualization and dynamical phase diagrams have been determined. The crystal-superfluid interface in aerogel advances via creep at high temperatures and avalanches at low temperatures. The transition temperature is higher at a higher interface velocity and lower in higher porosity aerogels. The transition is due to competition between thermal fluctuations and disorder for the crystallization process.

DOI: [10.1103/PhysRevLett.101.175703](https://doi.org/10.1103/PhysRevLett.101.175703)

PACS numbers: 64.70.D-, 67.80.-s, 81.10.-h

Freezing of a fluid in small pores is a common phenomenon in a natural environment [1]. It is known that water remains in a liquid phase even below 0°C when contained in a fine soil and freezes into ice at lower temperatures. However, this is sometimes a very complicated phenomenon and consists of several slow processes other than crystallization, such as a viscous fluid flow in pores and diffusion of latent heat. These hide intrinsic features of the crystallization in a quenched disorder by pores. Using low-temperature ^4He in the superfluid and the solid phases causes the flow in the pores to be fast enough to reveal the nature of crystallization dynamics. Here we report a novel dynamical transition of the crystallization of ^4He in pores. The crystal-superfluid interface advances via creep at high temperatures and via avalanches at low temperatures.

The reduction of freezing temperature is found in many fluids including superfluid ^4He when contained in various porous materials [2–5]. The use of low-temperature liquid and solid ^4He has an advantage over other materials since all impurities are frozen on a cell wall at cryogenic temperatures and do not enter the bulk ^4He . This makes precise measurements with ^4He possible, and this substance has thus been a model system for studying the dynamic and static properties of the crystal surface [6]. ^4He has a nearly temperature-independent crystallization pressure at about $P_0 = 25$ bar (or, equivalently, no release of the latent heat in the crystal-superfluid phase transition) below 1 K down to absolute zero. Therefore, one can study the crystallization dynamics in a wide temperature range without much change in other parameters and focus on the effect of the thermal fluctuations and the disorder on the crystallization. Avalanche has been observed in dynamics of various types of condensed matter [7–11] but not much is known in a real crystal growth process. A burstlike growth of dislocation-free ^4He crystals was reported below 200 mK [12].

As a porous material for the experiment we use silica aerogels [13–15]. Aerogel consists of silica beads of a few nm diameter. Aerogel has a very large open volume and its porosity ranges from 90 to 99.5% in volume. It introduces a quenched disorder to the phase transition of ^4He within it

[13–20]. We can alter the strength of the disorder broadly by choosing the porosity of the aerogel. Aerogel is very transparent and suitable for visualizing the dynamics within it.

Our sample cell is cooled by a ^3He - ^4He dilution refrigerator with optical access [21]. The cell has two variable-volume chambers; a high-pressure chamber (A) and a low-pressure chamber (B), part of which is made of bellows. Diameter of the bellows of chamber B is larger than that of chamber A, and the bellows are connected by a rigid rod as in Fig. 1(a). We are able to change the volume of chamber A even if it is filled with crystals by the low-pressure (P_B) liquid ^4He in chamber B. Chamber A has optical windows aligned in a straight line and its interior is observable from the outside of the cryostat. Aerogel (C) made by Marke Tech International Inc. [22] is installed on a stage fixed on the bottom of chamber A. Pressure (P) is measured by a capacitive pressure gauge mounted on the sidewall of chamber A. The pressurization rate \dot{P} of chamber A is adjusted by \dot{P}_B which is controlled by a needle valve of the gas handling system. We illuminated the chamber from

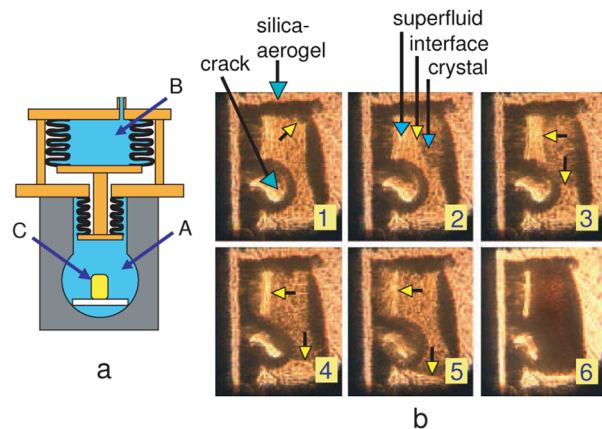


FIG. 1 (color online). (a) Schematics of the experimental cell. (b)1–5. Consecutive photographs of crystallization of ^4He in aerogel. Short (yellow) arrows indicate the position of the interface. The circle seen in the aerogel is an undesired crack of the aerogel. (b)6. Photograph during the melting. (See text.)

the back window by a parallel light (shadowgraphy), and recorded the image through the front window by a high-quality CCD camera.

The initial situation of the experimental sequence is such that chamber *A* is filled with ^4He at P_0 and that bulk crystals and superfluid liquid coexist in it. At this moment only the liquid exists in the aerogel. We start to pressurize chamber *B* continuously at a fixed rate \dot{P}_B and at a temperature T , and the bellows of chamber *A* expands. The bulk crystals grow in chamber *A* and eventually occupy the space outside of the aerogel completely. Thereafter, the pressure in chamber *A* increases above P_0 and crystallization in the aerogel begins at a particular pressure above P_0 . We record how the crystallization in the aerogel proceeds [Fig. 1(b) 1–5]. After the crystals fill the aerogel, we depressurize chamber *B* to the initial pressure. The crystals in the aerogel melt by the decompression and chamber *A* returns to P_0 . During the melting the clear interface is not observable but the aerogel becomes opaque [Fig. 1(b) 6]. The crystal starts to melt at the pressure lower than that in the crystallization case. We repeat this sequence at various \dot{P}_B and T to obtain the dynamical phase diagrams.

The crystallization process is shown in Fig. 1(b). In this example, porosity of the aerogel is 90.4%, temperature is 420 mK and $\dot{P}_B = 5$ mbar/s. We refer to this aerogel as P90 in this report; it is 8 mm in width, 13 mm in height and 12 mm in depth. At low P , only the superfluid exists in the aerogel and no interface is seen. At an overpressure of $\Delta P = P - P_0 \sim 2$ bar, the interface begins to appear in the aerogel from the upper right corner [Fig. 1(b) 1] and moves to the inside [Fig. 1(b) 2–5]. Eventually the aerogel is filled with the crystals at $\Delta P \sim 3$ bar. Pressure behavior was reported in Ref. [21] at 0.84 K and is essentially the same at all experimental temperatures. Uncertainty of the pressure is presumably a pressure inhomogeneity of the order of yielding stress of the crystal, a few 100 mbar at most. This inhomogeneity may be a cause of the preferential growth of the crystal from the upper right corner. Although we see only the projected image of the crystals in the aerogel, the interface proceeds at almost constant velocity in the initial stage of the crystallization and thus a projected mean velocity of the interface v is obtained. The velocity v is roughly proportional to the pressurization rate \dot{P}_B and is temperature independent.

The manner of crystallization in the aerogel at low temperatures (Ref. [23]) is quite different from that at high temperatures (Ref. [24]). Figure 2(a) shows the profile of the interface at intervals of 3 s at 850 mK and $\dot{P}_B = 10$ mbar/s. In this high temperature region, the interface appears irregular but advances smoothly at about $v \sim 50$ $\mu\text{m/s}$. We refer to this as a creep region in this report.

At lower temperatures, however, the interface motion becomes highly intermittent. It shows a slip-stick behavior and moves via avalanches. We refer to this as an avalanche region. Figure 2(b) shows the profile of the interface just after each separate avalanche at 420 mK and $\dot{P}_B = 5$ mbar/s. The scale of projected area of avalanches is

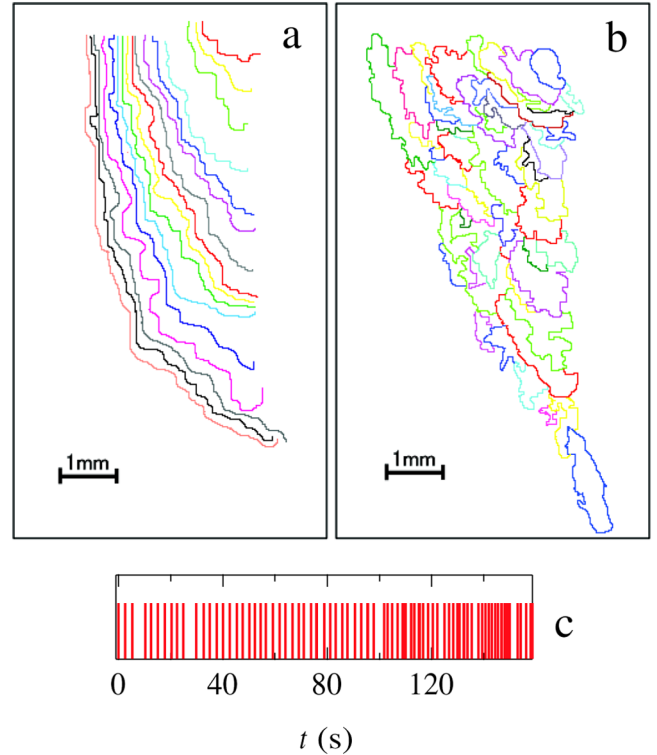


FIG. 2 (color online). Profiles of the crystal-superfluid interface in aerogel. (a) Creep region. (b) Avalanche region. (c) Avalanche sequence. (See text.)

0.2 to 1 mm^2 and the part of the interface other than the avalanche remains unmoved. This means that avalanches are macroscopic and local. Sequence of the avalanches is shown in Fig. 2(c); the vertical lines represent the time at which each avalanche event occurred in Fig. 2(b). Time intervals between the avalanches are a few seconds in the initial stage of the crystallization and become a little shorter in the later stages.

The avalanches seem to be random and not spatially correlated. The interface advances on the whole over a longer time scale than the intervals between the avalanches and we can also define the mean interface velocity v in the avalanche region as in the creep region. In Fig. 2(b), $v \sim 30$ $\mu\text{m/s}$. If we compare v at the same \dot{P}_B , the v roughly agree with each other in the two regions. In order to follow the interface position during an avalanche we also used a high-speed camera. The avalanches continue only for an order of 10 ms, during which the instant velocity is very high, ranging from 10 to 400 mm/s , about 4 orders of magnitude higher than v .

We determined the dynamical phase diagram of the crystallization in the aerogel at various temperatures and \dot{P}_B . In Fig. 3(a), we use v for the vertical axis since it has more intrinsic meaning than \dot{P}_B . Red squares (blue circles) mean that we observe avalanches (creep); yellow triangles are an intermediate case. Transition temperature is about 600 mK at low v ; below (above) this temperature, it is the avalanche (creep) region. From the observation alone it is

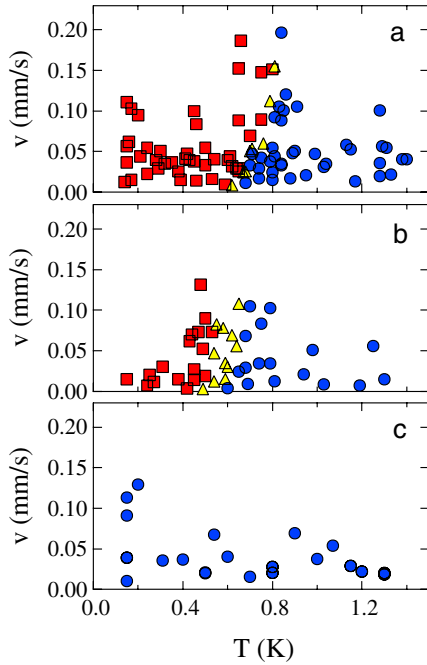


FIG. 3 (color online). Dynamical phase diagrams of the crystallization of ^4He in aerogels. The porosities of the aerogels are 90.4% (a), 95.8% (b), and 99.5% (c). Red squares (blue circles) indicate that avalanche (creep) of the interface was observed. Yellow triangles are the points where both avalanche and creep coexist.

difficult to conclude definitely whether this is a discontinuous phase transition or a crossover. However, the transition region looks rather sharp and no gradual increase of the avalanche size is seen in the creep region as approaching the transition. Furthermore, avalanche and creep coexist in the intermediate region (Ref. [25]). We interpret the transition as being discontinuous.

The transition line in the v - T graph has a finite slope and shifts to about 800 mK at high v . Compared to the avalanches at low v , these at high v are not spatially random and are more correlated. An avalanche at a particular position induces a succession of avalanches one after another, and the crystallization proceeds with a train of these avalanches (Ref. [26]). One probably must slowly compress the cell and wait long enough for the system to relax after an avalanche in order to have the random avalanches, otherwise the avalanches show correlations.

Phase diagrams are determined using the same procedure for higher porosity aerogels: 95.8% [Fig. 3(b)] and 99.5% [Fig. 3(c)]. We refer to the aerogels as P96 and P99. In P96, the transition temperature shifts to a slightly lower temperature than in P90, to about 500 mK at low v , and the intermediate region is a little wider. Other characteristics of the dynamical phase diagram are similar to those in P90. On the other hand, the highest porosity aerogel P99 has only the creep region down to our lowest temperature 150 mK and no avalanche is observed during the crystallization.

Overpressure required for the crystallization in the aerogels is about $\Delta P = 1$ bar for P96 and $\Delta P = 0.2$ bar for P99. ΔP can be used to make estimations of the effective pore radius R by the equation [2], $\Delta P = \frac{V_s}{V_l - V_s} \frac{2\alpha}{R}$, where V_s , V_l , and α are the molar volume of the solid and the liquid and the surface stiffness [6]. We obtain $R = 23$, 46, and 230 nm for P90, P96, and P99, respectively.

Aerogel provides disordered pinning potentials for the ^4He crystal on the scale of their pore size and the crystallization has to advance by overcoming the energy barriers. The overall features are qualitatively understandable as follows. At high temperatures, crystals are able to overcome the energy barriers by thermal activation and the crystal-superfluid interfaces are not pinned by the disorder. Although the crystallization appears to proceed smoothly on the macroscopic scale, it is probably successions of microscopic avalanches on the scale of the disorder. At low temperatures, however, thermal activation is too weak to crystallize in the aerogel. The interface will be strongly pinned and not able to move at all. Nevertheless, we continuously compress chamber A at a constant rate, and thus more and more stress is accumulated in the system by the compression. The energy barriers will decrease gradually with the compression and eventually disappear at a critical stress. Thereafter, crystallization advances abruptly via an avalanche, which releases the accumulated stress in a moment and recreates a large energy barrier quickly. By repeating this slip-stick process, the crystallization can proceed on the whole in the avalanche region. This argument, however, fails to explain the order of the transition. It is surprising that a small change in temperature can lead to the drastic change from creep to avalanche. This implies that a possible effective interaction between the interface and silica beads disappears steeply at the transition with warming due to the thermal fluctuation.

At higher \dot{P}_B , avalanches will be able to take over the creep at higher temperature and thus the transition temperature should rise at high v . Positive slope of the transition temperature is likely to occur. In higher porosity aerogels, the weaker disorder will make thermal activations possible at lower temperatures and the transition temperature should shift lower. If the diameters of silica beads do not depend on the porosity of the aerogels, pinning strength for each silica bead or strand should be independent of the porosity. The observed porosity dependence of the transition temperature implies that overall strength of the disorder depends on the density of silica strands and that the pinning is cooperative.

Similar transition from small to large avalanches was reported in the superconducting vortex avalanches as a function of temperature [9,10]. Size distribution was analyzed in the context of the self organized criticality [11]. We observe only the projected image of the 3D avalanche and are not able to analyze the size distribution in the present experimental setup. Quasi-2D configuration such as a thin aerogel between two glass plates will be useful for

studying the size distribution and is planned for a future experiment.

In the ordinary situation of bulk crystal growth, a fluid surrounds a crystal and mass is transported to its interface by the fluid through a flow or diffusion. The crystallization in porous materials is quite different. Bulk crystals surround the aerogel which is filled with a superfluid and the mass has to be transported by the crystal in order to have crystallization in the aerogel. The density of the crystal is about 10% greater than the superfluid. The way in which crystallization occurs in pores is not simple. One possibility is a crystal growth as follows. The bellows compresses the surrounding bulk crystals and its pressure or chemical potential becomes higher. Thus, crystals melt into the superfluid at the outer aerogel surface and enter the aerogel. The superfluid flows towards the interface in the aerogel through the pores and crystallizes there again. Another possibility is a penetration of the crystal itself via a plastic deformation through the pores in the aerogel. Although in a real situation both mechanisms may be involved and cannot be clearly separated, it is important to distinguish them to fully understand the crystallization dynamics and the dynamical transition in the aerogel.

It is also intriguing to know the surface structure of crystals in the aerogel. Since the aerogel is highly opaque during the melting, it is very likely that the crystals are in a highly polycrystalline state composed of μm size grains, as found by a recent observation of the melting process of ^4He polycrystals [27]. Invasion of the liquid into the grain boundaries between small crystals presumably causes the strong scattering of light during the melting. This is the reason that we see no sign of a macroscopic facet of the crystals in the aerogel even well below the roughening transition temperatures [6]. The size of each crystal is, therefore, much smaller than the avalanche size. A single avalanche is a creation of a large number of small crystals at once. This is very different from the crystal growth of a bulk ^4He crystal where the mobility of rough or facet surfaces governs the crystallization dynamics. In aerogel, the pinning plays a crucial role in crystal growth. It is still an open question whether the surface of the microcrystals is rough or faceted.

In summary, dynamical transition from a creep at high temperatures to an avalanche at low temperatures was observed in the crystallization of ^4He in aerogels by direct visualization. The competition between the thermal fluctuation and the quenched disorder is revealed in crystallization dynamics for the first time by the swift superflow through the small pores. Transition temperature is lower for higher porosity aerogels and higher at higher mean interface velocity.

We would like to thank Hiroshi Matsukawa for useful discussions. This study is supported in part by the Hosokawa Powder Technology Foundation, a 21st Century COE Program at Tokyo Tech “Nanometer-Scale

Quantum Physics”, a Grant-in-Aid for Scientific Research on Priority Areas (Grant No. 17071004) from MEXT Japan and by a “Ground-based Research Announcement for Space Utilization” promoted by the Japan Space Forum.

-
- [1] J. G. Dash, A. W. Rempel, and J. S. Wettlaufer, *Rev. Mod. Phys.* **78**, 695 (2006).
 - [2] E. D. Adams *et al.*, *J. Low Temp. Phys.* **66**, 85 (1987).
 - [3] K. Yamamoto, Y. Shibayama, and K. Shirahama, *J. Phys. Soc. Jpn.* **77**, 013601 (2007).
 - [4] M. Hiroi *et al.*, *Phys. Rev. B* **40**, 6581 (1989).
 - [5] T. Mizusaki, R. Nomura, and M. Hiroi, *J. Low Temp. Phys.* **149**, 143 (2007).
 - [6] S. Balibar, H. Alles, and A. Y. Parshin, *Rev. Mod. Phys.* **77**, 317 (2005).
 - [7] A. H. Wootters and R. B. Hallock, *Phys. Rev. Lett.* **91**, 165301 (2003).
 - [8] A. Prevost, E. Rolley, and C. Guthmann, *Phys. Rev. B* **65**, 064517 (2002).
 - [9] E. Altshuler and T. H. Johansen, *Rev. Mod. Phys.* **76**, 471 (2004).
 - [10] E. R. Nowak *et al.*, *Phys. Rev. B* **55**, 11 702 (1997).
 - [11] J. P. Sethna, K. A. Dahmen, and C. R. Myers, *Nature (London)* **410**, 242 (2001).
 - [12] J. P. Ruutu *et al.*, *Phys. Rev. Lett.* **76**, 4187 (1996).
 - [13] J. V. Porto and J. M. Parpia, *Phys. Rev. B* **59**, 14583 (1999).
 - [14] T. M. Haard *et al.*, *Physica (Amsterdam)* **284B**, 289 (2000).
 - [15] F. Detcheverry *et al.*, *Phys. Rev. E* **68**, 061504 (2003).
 - [16] T. Herman, J. Day, and J. Beamish, *Phys. Rev. B* **72**, 184202 (2005).
 - [17] T. Lambert *et al.*, *J. Low Temp. Phys.* **134**, 293 (2004).
 - [18] J. Yoon *et al.*, *Phys. Rev. Lett.* **80**, 1461 (1998).
 - [19] W. Miyashita *et al.*, *J. Phys. Chem. Solids* **66**, 1509 (2005).
 - [20] R. Nomura *et al.*, *Phys. Rev. E* **73**, 032601 (2006).
 - [21] A. Osawa *et al.*, *J. Low Temp. Phys.* **150**, 499 (2008).
 - [22] 4750 Magnolia Street, Port Townsend, WA 98368, USA.
 - [23] See EPAPS Document No. E-PRLTAO-101-022844 for crystallization in the avalanche region at low v in P90 (5 times faster). For more information on EPAPS, see <http://www.aip.org/pubservs/epaps.html>.
 - [24] See EPAPS Document No. E-PRLTAO-101-022844 for crystallization in the creep region at low v in P90 (5 times faster). For more information on EPAPS, see <http://www.aip.org/pubservs/epaps.html>.
 - [25] See EPAPS Document No. E-PRLTAO-101-022844 for crystallization in the intermediate region at low v in P90 (5 times faster). For more information on EPAPS, see <http://www.aip.org/pubservs/epaps.html>.
 - [26] See EPAPS Document No. E-PRLTAO-101-022844 for crystallization in the avalanche region at high v in P90 (real time). For more information on EPAPS, see <http://www.aip.org/pubservs/epaps.html>.
 - [27] S. Balibar and F. Caupin, *J. Phys. Condens. Matter* **20**, 173201 (2008).